Available online at www.sciencedirect.com
ScienceDirect
Spectrochimica Acta Part A 70 (2008) 458–461
SPECTROCHIMICA ACTA PART A
www.elsevier.com/locate/saa

# Oxygen *K*-edge XANES investigation of $Ni_cMg_{1-c}O$ solid solutions

Dongliang Chen [a], Jun Zhong [a], Xiang Wu [a], Ziyu Wu [a,*], Nina Mironova-Ulmane [b], Alexei Kuzmin [b], Augosto Marcelli [c]

[a] *Institute of High Energy Physics, Chinese Academy of Sciences, Beijing 100049, China*
[b] *Institute of Solid State Physics, University of Latvia, Kengaraga 8, LV-1063 Riga, Latvia*
[c] *Laboratori Nazionali di Frascati, Istituto Nazionale di Fisica Nucleare, 00044 Frascati, Italy*

Received 25 November 2005; accepted 23 November 2007

**Abstract**

A series of $Ni_cMg_{1-c}O$ solid solutions are characterized by means of synchrotron radiation X-ray diffraction and X-ray absorption near-edge-structure spectroscopy at oxygen *K*-edge (532 eV). A dramatic drop of the pre-edge peak intensity is observed in the $Ni_cMg_{1-c}O$ system upon dilution. It can be attributed to a decrease of $3d^8(Ni^{2+})$–$2p(O^{2-})$ mixing upon dilution with magnesium ions due to a decrease of the number of 3d vacancies as nickel ion is replaced by magnesium ion. Similarly, the decrease of the number of 4s and 4p vacancies also leads to a decrease of $4s4p(Ni^{2+})$–$2p(O^{2-})$ hybridization, and hence a drop of intensities of features B and C. The features E and F are more sensitive to the increase of the degree of disorder upon dilution than feature D, revealing that the latter is mainly dependent by the medium-range order.


*Keywords:* XANES; $Ni_cMg_{1-c}O$; Oxygen *K*-edge; Hybridization

## 1. Introduction

Diluted antiferromagnets represent an interesting class of materials, whose crystallographic structure is closely related to their magnetic properties [1]. The $Ni_cMg_{1-c}O$ solid solution is a prototype of a diluted face-centred-cubic (fcc) antiferromagnet whose magnetic properties vary with the composition from antiferromagnetic-like behaviour for pure NiO to diamagnetic-like behaviour for pure MgO [2,3]. The lattice constant $a$ of the $Ni_cMg_{1-c}O$ solid solution depends nearly linearly on the composition: it increases slightly upon dilution from 4.1773 Å in pure NiO to 4.2123 Å in pure MgO [4].

A single phase transition upon cooling from a paramagnetic-like to an antiferromagnetic-like state is observed for all compositions $c$ above the percolation threshold $c_p = 0.2$ for $Ni_cMg_{1-c}O$ [2,3]. Pure NiO belong to the group of type-II antiferromagnetic (AF2) charge-transfer insulators with the Néel temperature $T_N = 523$ K. The magnetic interactions in the fcc antiferromagnets are characterized by the relative signs and strengths of the nearest-neighbour (NN), $J_{NN}$, and the next-nearest-neighbour (NNN), $J_{NNN}$, superexchange interactions between two transition metal (TM) ions via an oxygen ion [5]. The exchange interactions $J_{NN}$ and $J_{NNN}$ are determined by the intermixing of the $3d^8(Ni^{2+})$ and $2p(O^{2-})$ states, which can be directly accessible by the X-ray absorption near-edge-structure (XANES) spectroscopy, being sensitive to a variation of the local electronic and atomic structures related mainly to site symmetry, interatomic distances, coordination numbers, thermal vibrations and static disorder. However, although the variation of the pre-edge peak at the Ni (Co) *K* absorption edge in $Ni_cMg_{1-c}O$ and $Ni_cCo_{1-c}O$ solid solutions upon dilution have been studied [6,7], the changes of hybridization between $3d^8(Ni^{2+})$ and $2p(O^{2-})$ states upon composition variation is still an open question in $Ni_cMg_{1-c}O$ solid solutions.

In the present work, we focus on the pre-edge peak variation at the O *K*-edge XANES in $Ni_cMg_{1-c}O$ solid solutions upon dilution. In particular, we address the composition dependence of $2p(O^{2-})$–$3d^8(Ni^{2+})$ states mixing by looking at the O *K*-edge, which should provide us with better resolution and higher sensitivity.

## 2. Experimental

The $Ni_cMg_{1-c}O$ solid solutions with $c = 0.99$, 0.90, 0.80, 0.65 and 0.55 were prepared as described briefly below, and

* Corresponding author.
*E-mail address:* wuzy@ihep.ac.cn (Z. Wu).

1386-1425/$ – see front matter © 2008 Elsevier B.V. All rights reserved.
doi:10.1016/j.saa.2007.11.032

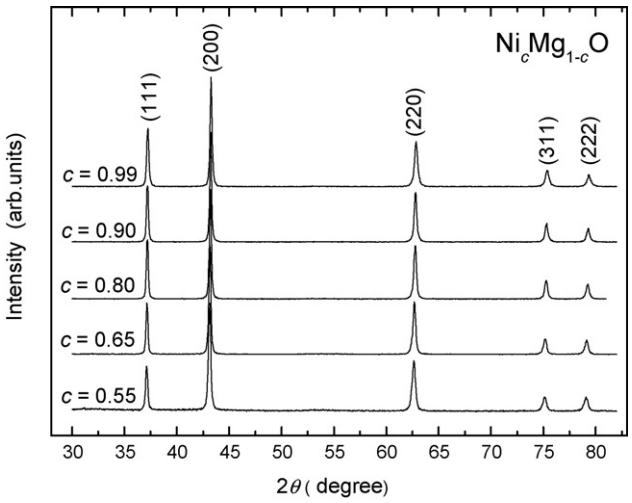


Fig. 1. XRD patterns of the $Ni_cMg_{1-c}O$ solid solutions with the compositions $c = 0.99$, 0.90, 0.80, 0.65 and 0.55.

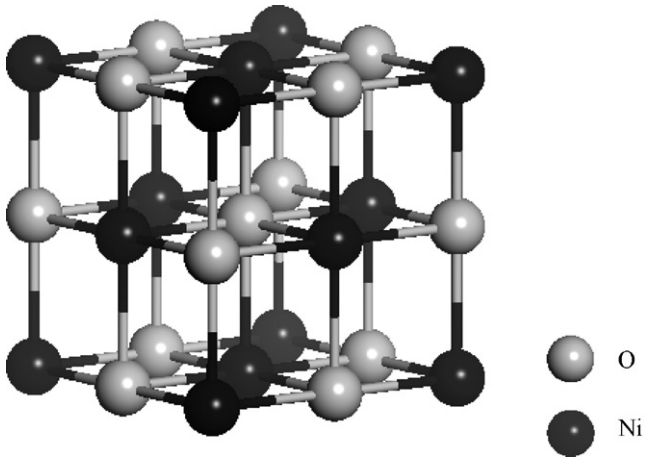


Fig. 2. Schematic NaCl-type structure of NiO with space group *Fm*-3*m*. Black balls represent nickel atoms and gray balls oxygen atoms.

the more detailed procedure can be found in Refs. [2,4]. The amounts of aqueous solutions of Mg $(NO_3)_2{\cdot}6H_2O$ and Ni $(NO_3)_2{\cdot}6H_2O$ salts corresponding to the appropriate solid solution composition were mixed and slowly evaporated. The remaining dry 'flakes' were heated up to 770–870 K to remove $NO_2$ completely. The polycrystalline solid solution obtained was powdered and annealed for 100 h at 1470 K in air and then quickly cooled down to the room temperature. X-ray structural and phase analyses were carried out to control the prepared samples [4].

Synchrotron radiation X-ray diffraction (XRD) characterization of the $Ni_cMg_{1-c}O$ solid solutions was carried out at the Beijing synchrotron radiation facility (BSRF) using the wavelength of 1.53989 Å. The XRD patterns were recorded at room temperature in the angular range of $2\theta = 30$–$82^\circ$ with a step scan of 0.04° and a counting time of 1 s/point.

The oxygen *K*-edge XANES experimental spectra of pure NiO and $Ni_cMg_{1-c}O$ solid solutions were recorded at the Beijing synchrotron radiation facility (BSRF) using the emitted light of the storage ring working at the typical energy of 2.2 GeV with an electron current of about 100 mA. Samples were loaded in an UHV chamber and maintained in a background pressure of $\sim 5 \times 10^{-8}$ Pa. Spectra were collected using the total electron yield (TEY) mode, a surface-sensitive detection method with a typical probing depth of a few nanometres. The experimental resolution at these photon energies was about 0.3 eV. More details on the experimental setup for the O *K*-edge experiments can be found in Ref. [8].

## 3. Results and discussion

The XRD patterns of $Ni_cMg_{1-c}O$ solid solutions with compositions $c = 0.99$, 0.90, 0.80, 0.65 and 0.55 are displayed in Fig. 1: they are in good agreement with the previous results reported in Ref. [3] and Ref. [4]. One can observed clearly that the (1 1 1) peak intensity in solid solutions drops monotonically with a decrease of the NiO content ($c$) due to the difference between the X-ray scattering intensities of the nickel and magnesium sublattices. The intensity of the (1 1 1) peak in $Ni_cMg_{1-c}O$ solid solutions, having the NaCl-type structure (Fig. 2), depends on the difference between the number of electrons of anions and cations [4]. The positions of (1 1 1), (2 0 0), (2 2 0), (3 1 1) and (2 2 2) peaks shift gradually toward to the lower $2\theta$ direction with the decrease of composition $c$, indicating an increase of the lattice constant in the $Ni_cMg_{1-c}O$ system. We underline here that the $Ni_cMg_{1-c}O$ solid solutions are single phase, and the lattice constant of the rock-salt structure is nearly linear with composition [4].

Fig. 3 displays the oxygen *K*-edge XANES spectra of pure NiO and a series of $Ni_cMg_{1-c}O$ solid solutions. All the spectra have been normalized using Cromer–Liberman calculations by IFFEFIT code [9,10]. The top curve corresponds to the O *K*-edge XANES spectrum of pure NiO and is in good agreement with previous data of Refs. [11–18]. The spectrum has six main features labelled by A, B, C, D, E and F, respectively. The other O *K*-edge XANES spectra in Fig. 3 are of $Ni_cMg_{1-c}O$ solid solutions with compositions $c = 0.99$, 0.90, 0.80, 0.65 and 0.55.

One can roughly divide the O *K*-edge XANES spectra into three regions. The first region (labelled A) is usually called the "pre-peak" located at about 532 eV. It can be seen clearly in Fig. 3 that the intensity of feature A reduces remarkably and monotonically with the decrease of composition $c$. The second region presents two strong features labelled B and C, respectively, displaying a broader structure about 10 eV above the edge. The intensities of feature B and C also drop upon the dilution with magnesium ions, and the feature B becomes a small shoulder of the peak C at $c = 0.55$. The third region spreads from 545 to 570 eV and contains three broad peaks labelled D, E and F, respectively. The shape, energy position and intensity of the feature D are independent upon dilution. With the decrease of the composition $c$, the feature E disappears gradually and the feature F broadens as well as its energy position shifts gradually toward low energy.

For the pure NiO, the feature A is a probe of transitions from O 1s electron to antibonding O 2p states hybridized with the 3d metal states, mainly localized at the Ni site. The intensity and shape of the feature A depend on the Ni site symmetry,

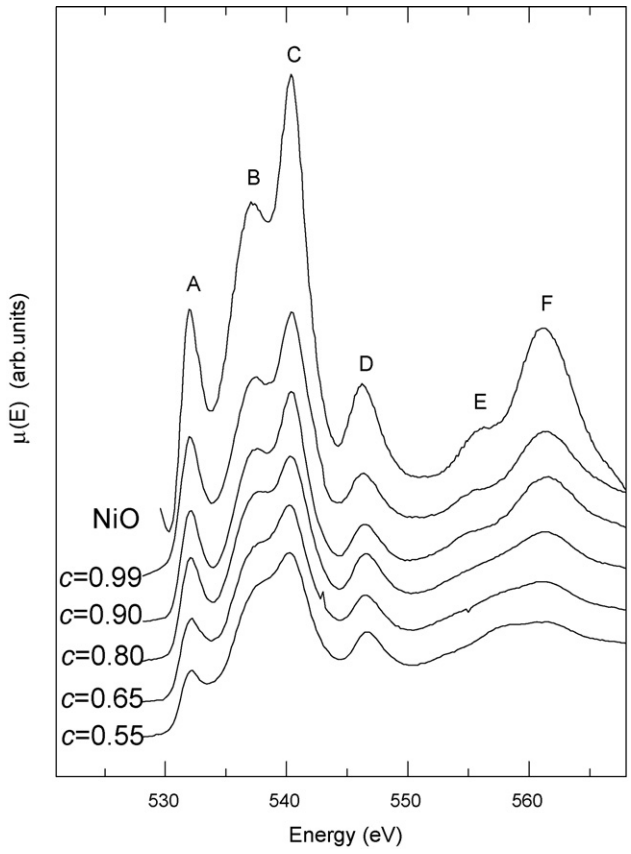


Fig. 3. Oxygen *K*-edge XANES spectra for polycrystalline NiO and $Ni_cMg_{1-c}O$ solid solutions with the compositions $c = 0.99$, 0.90, 0.80, 0.65 and 0.55.

the occupation number of the d levels, as well as the O–Ni bond length [19–22]. The feature A of $Ni_cMg_{1-c}O$ solid solutions in Fig. 3 is attributed to the oxygen 2p weight in states of predominantly Ni 3d character, and its intensity decreases dramatically in the $Ni_cMg_{1-c}O$ system upon dilution, revealing unambiguously that the $3d^8(Ni^{2+})$–$2p(O^{2-})$ mixing weakens continuously versus Mg dilution, similarly to the trend observed in the $Li_xNi_{1-x}O$ system [14]. This behaviour can be explained by a decrease of the number of 3d vacancies as nickel ion is replaced by magnesium ion upon dilution, and hence resulting in the decrease of hybridization of O 2*p* states with the Ni 3d states. Moreover, doping can also decrease the Ni site symmetry and increase the O–Ni bond length. The latter, for the $Ni_cMg_{1-c}O$ system, depends linearly by dilution, but its increase is very limited [6,7]. However, the changes of feature A induced by the changes of the Ni site symmetry and the O–Ni bond length are negligible effects if compared to the influence on feature A by the decrease of 3d vacancies increasing dilution. A similar result has been previously reported by Collix et al. [23]. Likewise, de Groot et al. [19] and Kurata et al. [20] have observed a monotone decrease of the intensity of feature A over the TM series as a function of the number of accessible empty d states.

Qualitatively, one might expect a similar explanation for the doping dependence of features B and C in the $Ni_cMg_{1-c}O$ system. For pure NiO, features B and C are assigned to oxygen 2p character hybridized with Ni 4s and 4p states [20]. Upon dilution, the decrease of the number of 4s and 4p vacancies also leads to a decrease of $4s4p(Ni^{2+})$–$2p(O^{2-})$ hybridization, and hence a drop of intensities of features B and C. In the language of multiple-scattering theory [21,22], feature B arises from long- and/or medium-range contributions, while feature C is due to multiple scattering (MS), up to infinite order, of the final state photoelectron in the cage of the first oxygen shell, so that it can be called "a scattering resonance". It is possible to demonstrate that the intrashell MS within the first oxygen shell may account for feature C, while outer shells, e.g., atoms at longer distance, contribute to feature B. Doping reduces the Ni site symmetry and distorts the local structure around the O or Ni atom, resulting in an increase of the disorder degree in the $Ni_cMg_{1-c}O$ system upon dilution, and hence decreases the intensities of the scattering resonance B and C. Recent MS simulations revealed that features D and E for pure NiO arise from long- and/or medium-range contributions due to single-scattering (SS) processes between the photabsorber and atoms belonging to higher neighbouring shells, while feature F is associated with single scattering events involving the nearest neighbour oxygen shell [22]. Looking at feature D, its shape, energy position and intensity are independent upon dilution, so that the O–O bond length does not change with $c$ in the compositional range 0.99 to 0.55, in good agreement with EXAFS data [6]. On the contrary, the feature E disappears gradually with dilution. It drops and broadens versus composition $c$, addressing a strong distortion of the local structure when $c$ goes from 0.99 to 0.55. Actually features E and F are more sensitive to the disorder degree versus dilution than feature D. Moreover, the energy position of features E shifts toward low energy, implying the increase of the lattice constant versus dilution, in good agreement with XRD data and with the local atomic structure around $Ni^{2+}$ ions probed by extended X-ray absorption fine structure (EXAFS) experiments [6,7].

## 4. Conclusion

In conclusion, both XRD and oxygen *K*-edge (532 eV) X-ray absorption spectroscopy measurements were performed at room temperature in the polycrystalline $Ni_cMg_{1-c}O$ solid solutions with the following compositions: $c = 0.99$, 0.90, 0.80, 0.65 and 0.55. The $Ni_cMg_{1-c}O$ samples are single phase with a rock-salt structure characterized by a lattice constant depending linearly by the composition. The variations of intensity and shape of the pre-peak feature A have been analyzed in terms of electronic properties and occupation number of the 3d band, site symmetry and bond lengths. While the pre-edge peak intensity drops dramatically in the $Ni_cMg_{1-c}O$ system versus dilution, a behaviour assigned to a decrease of the $3d^8(Ni^{2+})$–$2p(O^{2-})$ mixing induced by the amount of magnesium ions replacing Ni, e.g., due to a decrease of the number of 3d vacancies. We have also investigated the MS spectral features above the pre-peak, namely the B, C, D, E and F features correlated to the medium and long range structural order. Upon dilution, the decrease of the number of 4s and 4p vacancies also leads to a decrease of $4s4p(Ni^{2+})$–$2p(O^{2-})$ hybridization, and hence to a drop of the intensities of features B and C. Features E and F are more sensi-

tive to the increasing degree of disorder upon dilution than that of feature D, mainly sensitive to the medium-range order. Moreover, the energy position of features E slightly shifts toward low energies, in agreement with the increase of the lattice constant in the $Ni_cMg_{1-c}O$ system upon dilution.

## Acknowledgements

This project was supported by the Key Important Nano-Research Project (No. 90206032) of the National Natural Science Foundation of China, the Outstanding Youth Fund (No. 10125523) and the Knowledge Innovation Program of the Chinese Academy of Sciences (KJCX2-SW-N11).

## References

[1] J.K. Furdyna, J. Kossut (Eds.), Diluted Magnetic Semiconductors, Academic Press, New York, 1988.
[2] A.Z. Menshikov, Yu.A. Dorofeev, A.G. Klimenko, N.A. Mironova, Phys. Status Solidi (B) 16 (1991) 275.
[3] Z. Feng, M.S. Seehra, Phys. Rev. B 45 (1992) 2184.
[4] A. Kuzmin, N. Mironova, J. Phys.: Condens. Matter 10 (1998) 7937.
[5] M.D. Towler, N.L. Allan, N.M. Harrison, V.R. Saunders, W.C. Mackrodt, E. Aprà, Phys. Rev. B 50 (1994) 5041.
[6] A. Kuzmin, N. Mironova, J. Purans, A. Rodionov, J. Phys.: Condens. Matter 7 (1995) 9357.
[7] A. Kuzmin, N. Mironova, J. Purans, J. Phys.: Condens. Matter 9 (1997) 5277.
[8] F.Q. Liu, K. Ibrahim, H.J. Qian, Y. Yang, X.P. Tao, J.F. Jia, Y.H. Dong, J. Electron Spectrosc. Relat. Phenom. 80 (1996) 409.
[9] M. Newville, J. Synchrotron Rad. 8 (2001) 322.
[10] D.T. Cromer, D. Liberman, J. Chem. Phys. 53 (1970) 1891.
[11] L.A. Grunes, R.D. Leapman, C.N. Wilker, R. Hoffmann, A.B. Kunz, Phys. Rev. B 25 (1982) 7157.
[12] I. Davoli, A. Marcelli, A. Bianconi, M. Tomellini, M. Fanfoni, Phys. Rev. B 33 (1986) 2979.
[13] S. Nakai, T. Mitsuishi, H. Sugawara, H. Maezawa, T. Matsukawa, S. Mitani, K. Yamasaki, Fujikawa, Phys. Rev. B 36 (1987) 9241.
[14] P. Kuiper, G. Kruizinga, J. Ghijsen, A. Sawatzky, H. Verweij, Phys. Rev. Lett. 62 (1989) 221.
[15] S.L. Dudarev, G.A. Botton, S.Y. Savrasov, C.J. Humphreys, A.P. Sutton, Phys. Rev. B 57 (1998) 1505.
[16] M. Finazzi, N.B. Brookes, Phys. Rev. B 60 (1999) 5354.
[17] S.L. Dudarev, M.R. Castell, G.A. Botton, S.Y. Savrasov, C. Muggelberg, G.A.D. Briggs, A.P. Sutton, D.T. Goddard, Micron 31 (2000) 363.
[18] C. Mitterbauer, G. Kothleitner, W. Grogger, H. Zandbergen, B. Freitag, P. Tiemeijer, F. Hofer, Ultramicroscopy 96 (2003) 469.
[19] F.M.F. de Groot, M. Grioni, J.C. Fuggle, J. Ghijsen, G.A. Sawatzky, H. Petersen, Phys. Rev. B 40 (1989) 5715.
[20] H. Kurata, E. Lefevre, C. Colliex, R. Brydson, Phys. Rev. B 47 (1993) 13763.
[21] Z.Y. Wu, S. Gota, F. Jollet, M. Pollak, M. Gautier-Soyer, C.R. Natoli, Phys. Rev. B 5 (1997) 2570.
[22] Z.Y. Wu, C.M. Liu, L. Guo, R. Hu, M.I. Abbas, T.D. Hu, H.B. Xu, J. Phys. Chem. B 109 (2005) 2512.
[23] C. Colliex, T. Manoubi, C. Ortiz, Phys. Rev. B 44 (1991) 11402.